# ON THE DEVELOPMENT OF
# CHITOSAN-*GRAFT*-POLY(N-ISOPROPYLACRYLAMIDE) BY
# RAFT POLYMERIZATION TECHNIQUE

CATALINA NATALIA CHEABURU-YILMAZ

*Department of Physical Chemistry of Polymers,*
*"Petru Poni" Institute of Macromolecular Chemistry, Iasi, Romania*
✉ *Corresponding author: duncaty@gmail.com*

The present paper aimed the synthesis of a functional biopolymer based on chitosan-*graft*-poly(N-isopropylacrylamide) (CS-*g*-PNIPAAm) using the "grafting from" technique *via* reversible addition-fragmentation chain transfer (RAFT) polymerization. Two different chain transfer agents, both compatible with the acrylic monomer were used. All intermediary products obtained from each step of chemical synthesis were quantified by ATR-FT-IR, ^{1}H-NMR and elemental analysis. Thermal properties confirmed that, with the chemical modification, chitosan structures became more complex and more thermally stable. The grafting efficiency was quantified as 40% and the final copolymer had double functionality, free amino groups and PNIPAAm segments on the side chains. Thanks to this, water solubility, pH and temperature sensitivity were achieved. The particle size of the aqueous solutions increased from 500 nm to 3.5 μm, with the increase of temperature from 25 to 50 °C. The lower critical solution temperature (LCST) of the solution was determined as 38-42 °C. CS-*g*-PNIPAAm could be used as a polymeric carrier within a pharmaceutical formulation for topical applications.

*Keywords*: chitosan, RAFT polymerization, poly(N-isopropylacrylamide), pH and temperature responsive, topical

## INTRODUCTION

Reversible addition–fragmentation chain transfer (RAFT) polymerization was reported as being a versatile "living" radical technique, which involves a fast, reversible chain-transfer process of a compound reacting with propagating chain radicals. The process has no metal contamination, and is applicable to a wide range of monomers and reaction conditions.[1,2] The diversity of properties of the smart polymers with linear structures, including responsive behavior of the functional side groups to pH, temperature, ionic strength, electric or magnetic fields, and light, reversible crosslinking *via* non-covalent bonds that can break and reform under certain external conditions, highlight the importance of of chemical modifications.[3]

As known, chitosan, with its structural specificity of having a linear β-1,4 linked glucosamine backbone, has become of interest for producing smart bio-polymers.[2-5] Its hydroxyl groups and one primary amino group in the repeating glycosidic residue act as reactive sites for a wide range of side-group attachments, including RAFT polymerization.

In the last decade, efforts have been made to functionalize chitosan *via* controlled radical polymerization methods, such as RAFT, atom transfer radical polymerization (ATRP), *etc*. RAFT polymerization of chitosan with various monomers has been reviewed recently.[2,3] Argüelles-Monal[3] reported various grafting techniques for chitosan, "grafting from" and "grafting onto" being the most relevant ones due to the fact that the polysaccharide's molecule is already established as main chain. Cheaburu-Yilmaz *et al*.[2] explored the possibilities to "graft from" various monomers on chitosan at the hydroxyl group from C6 of the polysaccharide chain's unit. By using a chain transfer agent (CTA), two alternative routes were reported. The first pathway was *via* esterification of the chain transfer agent (CTA) on the O-group of $C_6$ of the

phthaloylated chitosan, forming a macro-RAFT intermediary; the RAFT *in situ* polymerization of the monomer was performed in a second step. The second route included the attachment of the previously synthesized RAFT homopolymer on N-protected chitosan.[2] The success of the RAFT polymerization was directly dependent on the selection of the chain transfer agent (CTA) suitable for the monomer type and reaction conditions.[2-6] An inadequate selection of the RAFT agent may lead to loss of control of the reaction, prolonged retardation and induction periods or inhibition of polymerization. The Z and R groups of the RAFT agents represent the key factors of selection, since they influence the initiation and compatibility of the generated radicals with the specific monomer used for the polymerization.

Chitosan graft copolymers were synthesized by a couple of groups by using various types of CTA agents.[7-12] The strategy of *in-situ* polymerizing the monomers (*e.g.* PNIPAAm, acrylic acid, tosylic acid, *etc.*) in the presence of chitosan macro-RAFT intermediaries seemed to be the most convenient, taking into account how difficult it is to control the chemical modification of chitosan to obtain functional graft copolymers, *e.g.* stimuli responsive.

The present paper aimed at the synthesis of functional biopolymers based on chitosan-*graft*-poly(N-isopropylacrylamide), using the "grafting from" technique. The used approach was to establish the most facile way to obtain a functional chitosan with water solubility, and pH and temperature responsive moieties on the side groups. By combining the outcomes already found in the literature, this paper brings a contribution not only with an improved eco-friendly synthesis strategy, but also by the physical-chemical characterization of the product. Two different CTA agents were used, giving more alternatives to follow-up studies on chitosan-*graft*-PNIPAAm copolymers and

highlighting the potential of this functional copolymer for industrial use.

## EXPERIMENTAL
### Materials

For the experiments, chitosan of medium molecular weight (Sigma Aldrich product, 75-85% deacetylated), phthalic anhydride (PhA, ≥99%), N-isopropylacrylamide (NIPAAm, 97%), N,N-dicyclohexylcarbodiimide (DCC), 4-(dimethylamino)pyridine (DMAP, 99%), methanol (HPLC grade) and diethylether (extra pure) were purchased from Sigma-Aldrich and were used as received. 4,4-Azobis(4-cyanovaleric acid) (ACVA, 98%, Sigma) was used as initiator. N,N-Dimethylformamide (DMF, 99% Sigma), used as reaction medium, was dried on 4A molecular sieves and distilled under vacuum. The carboxyl-end functional RAFT agents used as chain transfer agents were: 4-cyano-4-(phenylcarbonothioylthio) pentanoic acid (CTA1), >97% (HPLC grade), and 4-cyano-4-(dodecylsulfanylthiocarbonylsulfanyl) pentanoic acid (CTA2). The structures of the two CTA agents are presented in Figure 1.

### Synthesis procedures
#### Preparation of phthaloylated chitosan

The protection of chitosan at $C_2$ was intensively studied and verified by various methods to be *via* phthaloylation of $NH_2$ group. Cheaburu-Yilmaz *et al.*[2] summarized the information found on the mechanism and various reaction conditions applied. The phthaloylation of chitosan was performed by a modified method by Kurita[13] to obtain a higher reaction yield. For this purpose, phthalic anhydride in excess (5.5 mmol) was first dissolved in 6 mL of $DMF/H_2O$ (95/5 v/v %) and added into a 2 neck-balloon, followed by the addition of chitosan powder in 1.86 mmol. The system was closed and purged by $N_2$ for 30 min to remove dissolved $O_2$. The solution was heated up to 120 °C and kept for 8 h for a complete reaction. The final brownish product was obtained by precipitation from ice-water and washing with methanol repeatedly.

The efficiency of the N-phthaloylation of chitosan was evaluated by FT-IR and elemental analysis, and the degree of substitution was calculated.
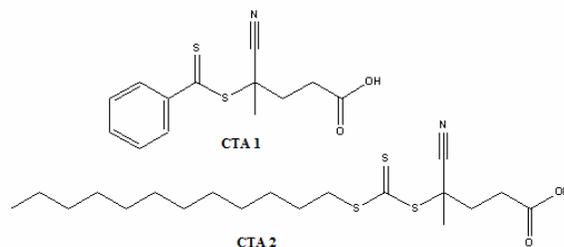


Figure 1: Chemical structure of the two RAFT agents (or CTA) used for the reaction

## Esterification of CTA agent on chitosan

The phthaloylated chitosan (CS-Ph) (1 mmol) was mixed with 1.2 mmol CTA in 30 mL of dried DMF in the presence of carbonyl activating reagents of DCC (1 mmol) and 4-DMAP (0.12 mmol) as catalysts. The reaction took place at room temperature for a pre-determined reaction time of 10 days. Preliminary studies were done for optimization of the reaction by verifying, qualitatively, the FT-IR spectra of purified products, and quantitatively, by calculating the reaction yield. The longer the reaction time, the higher the esterification yields achieved.

The obtained chitosan macro-RAFT agent had either reddish or yellowish color, as a function of the CTA agent used. The chitosan macro-RAFT agent (CS-CTA) was isolated by precipitation from ice water and then by refluxing for 5-8 h in a Soxhlet extractor with acetone. The reaction scheme of the esterification of phthaloyl chitosan using CTA 1 is presented in Figure 2. The obtained esterified product was further used as a macro-RAFT agent for the *in-situ* polymerization of NIPAAm.

When CTA2 was used, the reaction theoretically followed the same mechanism, except for the steric effect, which may take place between the macromolecular chains.

## Preparation of grafted copolymers

A selected amount of CS-CTA (0.0468 g, 0.05 mmol trithio groups) and dry DMF (5 mL) was stirred under nitrogen atmosphere. After complete dissolution, the initiator (ACVA) (0.01 mmol) and NIPAAm monomer (0.50 g; 4.4 mmol) were added. The polymerization reaction was conducted at 70 °C for 48 h. After the polymerization, the reaction mixture was precipitated in 10-fold diethyl ether and centrifuged at 3000 rpm at 4 °C for 15 min. The product (PhCS-*g*-PNIPAAm) was dried in a vacuum oven at 40 °C and the monomer conversion (Conv%) was calculated based on Equation (1):

$$Conv\% = \left(\frac{W_P - W_0}{W_M}\right) * 100 \tag{1}$$

where $W_P$, $W_0$ and $W_M$ are the weights of the copolymer, CS-CTA and monomer, respectively. The homopolymer was removed from the prepared copolymer by exhaustive extraction with acetone for 5 h. Purified copolymers were dried in a vacuum oven at 40 °C to constant weight. The graft content (G%) was calculated according to Equation (2):

$$G\% = \frac{(W_g - W_0)}{W_g} * 100 \tag{2}$$

where $W_g$ and $W_0$ are the weights of the graft copolymer and CS-CTA, respectively.

The structure of the obtained materials was confirmed by ATR-FTIR and ^{1}H-NMR spectra.

## Deprotection of phthaloyl groups

Deprotection of phthaloylated graft copolymers was necessary to be carried out on the synthesized chitosan derivatives (PhCS-*g*-PNIPAAm) to remove the phthaloyl moieties. This was an important step as free $NH_2$ groups of chitosan are the segments responsible for various properties, such as responsiveness to pH, antimicrobial action, gelling ability, *etc*. For this purpose, 100 mg of PhCS-*g*-PNIPAAm was mixed with 10 mL hydrazine monohydrate at 80 °C for 16 h under $N_2$ flow. Then, the solution was precipitated in 250 mL ice water. The product was collected by centrifugation at 4000 rpm, 4 °C for 20 min, washed with ethanol and extra-purified in a Soxhlet extractor with ethanol for 3-4 h (2-3 cycles). The product was collected, dried in a vacuum oven at 40 °C and subjected to FTIR analysis to confirm the structure.

## Characterization methods
### FTIR spectroscopy

ATR-FTIR spectroscopy was performed by using a Perkin Elmer Spectrum-100 instrument through reflexion on a diamond crystal with an angle of 45 degrees, with a resolution of 4 $cm^{-1}$ in the range of 450-4500 $cm^{-1}$.

### Elemental analysis

Elemental analyses were performed by Leco TruSpec Micro CHNS (Leco, St. Joseph, MI, USA). The experimental and theoretical ratios of C/N were determined and compared. The degree of substitution and the yields were also determined.

### Proton nuclear magnetic resonance ($^1$H-NMR) spectroscopy

The nuclear magnetic resonance ^{1}HNMR spectra were recorded using a AS400 Mercury Plus NMR Varian (Varian Inc., Palo Alto, CA, USA) (400 MHz) in deuterated DMSO and $D_2O$.

### Differential scanning calorimetry (DSC)

For differential scanning calorimetry, a Perkin Elmer DSC-8000, Waltham, MA instrument was used to examine the thermal behaviour of the products. The samples were sealed in aluminium pans and placed in the DSC equipment. DSC analysis was conducted under nitrogen flow (20 mL/min), within a temperature range of 30 and 300 °C, at a heating rate of 10 °C/min.

### Thermogravimetric analysis (TGA)

Thermogravimetry was performed by using a Perkin Elmer TGA 4000 device to evaluate the thermal degradation process of the samples. The temperature program was set from 30 to 500 °C, with a heating rate of 10 °C/min under $N_2$ flow.

### Particle size analysis

The particle size and polydispersity index (PDI) of the 0.2% polymer solutions in distilled water were determined using the light scattering method, with a Malvern Zetasizer 1000 HS (Malvern Instruments, England). The responsive behaviour was verified by

measuring the particle size of the formed suspensions, within the temperature range from 25 to 41 °C. The temperature range was selected on the basis of PNIPAAm characteristics, as its LCST is known to be of 32 °C. The LCST of the polymer solutions was determined by applying the sigmoidal mathematical model to the obtained results.
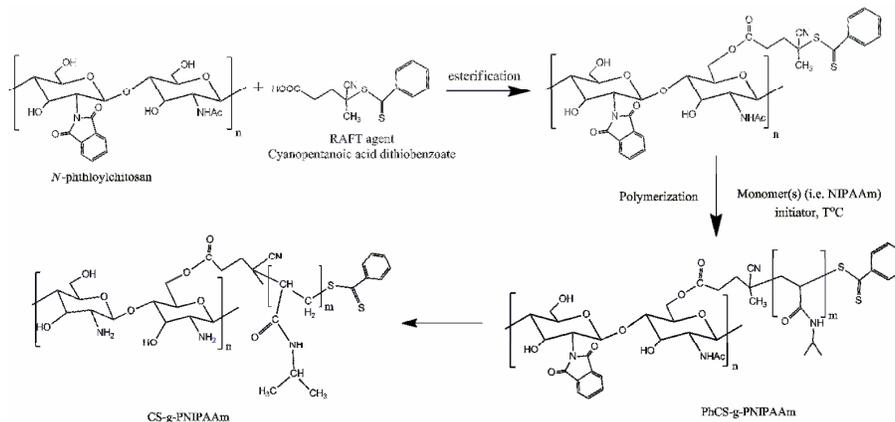


Figure 2: General mechanism to obtain CS-*g*-PNIPAAm graft copolymer using CTA as chain transfer agent

### *Gel permeation chromatography (GPC)*

The average molecular weight and polydispersity index of PNIPAAm homopolymers were determined by a Malvern aqueous gel permeation chromatography system (GPC). The device consists of one guard column and two ultra-hydrogel columns (10.000 Da and 1.000.000 Da), one refractive index detector with a peristaltic vacuum pump. 0.1 M $NaNO_3$ and 0.5% $NaN_3$ aqueous solutions were used as the mobile phase, with a flow rate of 0.7 mL/min, during the measurements. The calibration curve used in the measurements was prepared using 12 different poly(ethylene oxide) standards with peak molecular masses ($M_p$) ranging from 195 to 610.000 Da. Before the measurement, polymer solutions of 2 mg/mL concentration were dissolved in the GPC eluent and shaken for at least 6 hours to obtain complete dissolution. Then, the samples were filtered through 0.45 μm injector filters and measured for determining their number average molecular weight ($M_n$), weight average molecular weight ($M_w$), molecular weight distribution and polydispersity index (PDI).

### RESULTS AND DISCUSSION
### Functionalized chitosan with phthalic anhydride

The phthaloylation of chitosan was verified by ATR-FTIR and the spectra of the components and N-phthaloylated chitosan are given Figure 3.

In the FT-IR spectra, the characteristic peaks of pure chitosan were observed at 2921-2887 cm$^{-1}$, 1636 cm$^{-1}$, 1548 cm$^{-1}$, 1655 cm$^{-1}$ and 1068-1020 cm$^{-1}$ due to the stretching vibrations of –CH (-CH$_3$, -CH$_2$), C=O, -NH of secondary amide, amidic band I, and C-O of saccharide moiety. The structure of N-phthaloylated chitosan could be evidenced by the presence of characteristic bands for phthalic anhydride observed at 1778-1760 cm$^{-1}$, which corresponds to the formation of imide 5-atoms ring ($\upsilon$CO-N-CO) and phthalic anhydride at 1770-1850 cm$^{-1}$.

Additionally, the obtained derivative was investigated by elemental analysis to determine the substitution degree from the C/N ratio. The results obtained from elemental analysis were summarized in Table 1. As shown in Table 1, a degree of substitution of 92% was obtained by comparing the theoretical values of the C/N ratio with the experimental ones.

The structure of phthaloyl chitosan as main precursor for all other reactions was also verified by ^{1}H-NMR spectroscopy (Fig. 7). From ^{1}H-NMR spectra, the signals observed at 3.3, 3.9-4.5 and 4.9 ppm could be assigned to H$_2$, H$_{3-6}$ and H$_1$ of pyranose repeat units in CS. The aromatic phthalimide peaks of PhCS were observed at 7.2-8.0 ppm.[14]

### Grafted copolymers, chitosan-graft-PNIPAAm

The grafting reaction was performed *via* two steps, particularly the esterification of functionalized chitosan with CTA agent and the second step, the polymerization of the NIPAAm

monomer in the presence of the chitosan-macro RAFT intermediary.

**Esterification of CTA agents on phthaloylated chitosan**

The carboxyl containing CTA was bound to phthaloylated chitosan *via* esterification, and chitosan-CTA intermediary was obtained, herein referred to as PhCS-macro CTA or ester E1/E2.

The IR spectra of PhCS macro-CTAs are presented in Figure 4.

The FTIR spectra of PhCS macro-CTA show C=O stretching vibration at 1730-1770 $cm^{-1}$ due to the ester group, an aromatic bending vibration at 710 $cm^{-1}$ and -CH stretching of the alkyl groups between 2800-2900 $cm^{-1}$, confirming the success of the esterification of CTA to the polysaccharide backbone.



Figure 3: ATR-FT-IR spectra of phthaloylated chitosan and the pure constituents

Table 1
Elemental analysis results

| Sample | Experimental | | | Theoretical content | | | C/N ratio* | |
| | N (%) | C (%) | H (%) | N (%) | C (%) | H (%) | Exp. | Theoretical |
|---|---|---|---|---|---|---|---|---|
| Chitosan | 7.41 | 40.17 | 7.20 | 7.43 | 40.92 | 6.13 | 5.41 | 5.51 |
| Phtaloylated chitosan | 5.76 | 53.36 | 5.30 | 5.36 | 54.12 | 4.92 | 9.26 | 10.08 |

*DS = 92%

The efficiency of esterification was also confirmed by ^{1}H-NMR spectroscopy. The presence of the RAFT agent was demonstrated by the presence of the peak at 7.8 ppm, which could be assigned to the aromatic moiety of the RAFT molecule. By comparison with the spectra of pure chitosan, phthaloyl chitosan (PhCS) and the synthesized esters, their resonance peaks could be observed.

By comparing the two obtained esters of chitosan E1 and E2, similar structural characteristics were found. However, different peak intensities were observed due to the different Z- and R-groups of the CTA agents. The small

difference in intensities may lead to different steric stability and initiation speed. The R-group of the CTA agents was found to influence the stability of the radicals and the re-initiation process, as Rodrigues-Sanchez *et al.*[15] found out in their theoretical calculations, by means of the density functional theory.

To evaluate the efficiency of CTA agents, RAFT homopolymerization of NIPAAm was performed, applying the same reaction conditions. It was established that, by increasing the monomer/RAFT ratio and initiator concentration, the experimental molar mass might approach the theoretical value; hence, controlling the reaction time was additionally considered. The FTIR

spectra of PNIPAAm RAFT polymers (Fig. 5) show the main characteristic vibration bands of NIPAAm, CTA and PNIPAAm synthesized by RAFT. The reaction was found to be optimimum at 70 °C and a pre-determined time of 48 h for a better yield. The polydispersity index values for the homopolymers ranged between 1.2-1.4, showing a good control over the molecular weight of PNIPAAm polymers.

From the spectra, the C–H stretching region has three prominent peaks at approximately 2973 $cm^{-1}$ (isopropyl –$CH_3$ asymmetric stretch), 2934 $cm^{-1}$ (acrylamide backbone –$CH_2$ asymmetric stretch), and 2876 $cm^{-1}$ (isopropyl –$CH_3$ symmetric stretch). The amide region has two strong peaks at approx. 1632 $cm^{-1}$ (amide I) and 1538 $cm^{-1}$ (amide II). The C–H deformation region has peaks at 1459 $cm^{-1}$ (asymmetric deformation of isopropyl –$CH_3$), and 1387 $cm^{-1}$ and 1367 $cm^{-1}$ (both symmetric deformation of isopropyl –$CH_3$). In addition, the peak shown in the spectrum of the monomer at 1620 $cm^{-1}$, due to the absorption of the -C=C-vinyl group, disappeared from the spectra, demonstrating the success of polymerization and purification.

The molecular mass distribution of the formed PNIPAAm homopolymers was measured by GPC and the results were summarized in Table 2. This analysis was necessary as the control over the *in-situ* polymerization of NIPAAm under the used reaction conditions was hard to achieve.

GPC analysis showed that, experimentally, the obtained molar masses were close to the theoretical $M_n$ values (8000 Da). The polydispersity index values (PDI) ranged between 1.2-1.4, showing a reasonable control over the molecular weight of PNIPAAm polymers. On the other hand, CTA1 seemed to have better control on the polymerization of NIPAAm. Additionally, a conversion of the PNIPAAm-CTA homopolymers of 40% was found, showing that, apart from simple PNIPAAm homopolymers, which are preferentially formed, homopolymerized PNIPAAm was also formed also in the presence of CTA.

**Structural characterization of CS-*g*-PNIPAAm graft copolymers**

Grafting efficiency was evaluated by FT-IR and $^1$H-NMR spectroscopy. As shown in Figure 6, the FT-IR spectra of CS-*g*-PNIPAAm comprised the characteristic vibration bands of both the ester and the polymer.
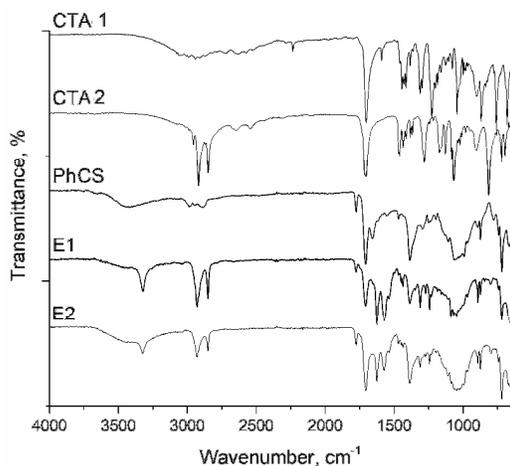


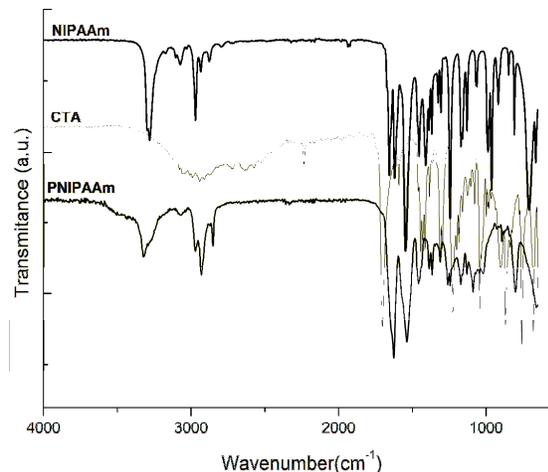Figure 4: ATR-FT-IR spectra of phthaloyl chitosan, CTA agents and synthesized esters



Figure 5: ATR-FT-IR spectra of NIPAAm monomer and its homopolymer (PNIPAAm)

Table 2
Average molecular weight values of PNIPAAm homopolymers

| Sample | $M_w$ (Da) | $M_n$(Da) | PDI |
|---|---|---|---|
| PNIPAAm-CTA1 | 7399 | 5903 | 1.25 |
| PNIPAAm-CTA2 | 5900 | 4200 | 1.40 |

The characteristic peaks at 1454 cm$^{-1}$ (–CH$_3$) and 1641 cm$^{-1}$ (O=C) showed the presence of PNIPAAm moieties. In addition, the absorption band around 3310 cm$^{-1}$ became wider, indicating hydrogen bond formation between –OH and –NHCO groups. These results further demonstrated the successful synthesis of CS-*g*-PNIPAAm.

As may be noted in Figure 6, the characteristic vibration band of phthaloyl groups from 1760 cm$^{-1}$ disappeared, as the deprotection with hydrazine took place, leaving just the characteristic vibration bands of chitosan and PNIPAAm.

$^1$H-NMR analysis also confirmed the successful polymerization of NIPAAm by using the chitosan macro-CTA agent. The $^1$H-NMR spectra of PhCS-*g*-PNIPAAm are shown in Figure 7. The peaks at 3.3, 3.9-4.5 and 4.9 ppm are assigned to H$_2$, H$_{3–6}$ and H$_1$ of pyranose repeated units in CS. The aromatic phthalimide peaks of PhCS appear at 7.2-8.0 ppm.[16] The signals of H-4, H-5, H-6 of chitosan were rather weak and could not be fully resolved because of overlapping with those of PNIPAAm, except for a typical peak of the proton on the carbon bearing the amino group (H2, 3.3 ppm) with a shift to the right side (2.4 ppm), which can also be found in the spectrum of PhCS. The graft copolymer not only shows the original signals of chitosan, but also has new peaks of PNIPAAm side chains. The signals at 1.2, 1.6, 1.8, 4.0 and 6.4 ppm could be assigned to PNIPAAm side chains.

Structural characterization revealed a main polymer chain with free amino groups and PNIPAAm moieties on the side groups. In terms of practical aspects, the obtained polymer should exhibit water solubility, pH sensitivity due to the -NH$_2$ groups and temperature response thanks to the PNIPAAm segments.

**Thermal characterization of graft copolymers**

Thermal characterisation of the pure and synthesized polymers was performed by means of thermogravimetry (TGA) and differential scanning calorimetry (DSC). Figure 8a and b presents the TGA and DTGA curves of the esters and grafted copolymers. From the curves, chitosan and phthaloyl chitosan showed two degradation steps: in chitosan, an 8% weight loss was found, associated with moisture loss at about 53 °C, which shifted to higher temperature up to 100 °C as the structure became more complex. The degradation of the polysaccharide chains occurs at about 307 °C.

Phthaloyl chitosan showed 2 main degradation steps: at 235 °C and 378 °C, showing better thermal stability in comparison with pure chitosan. By esterification of phthaloyl chitosan with RAFT agents, the formed intermediary showed 3 degradation steps: except the water loss in the first interval, 2 more degradation temperatures were determined: around 232 °C for E$_1$ and 233 °C for E$_2$, which can be due to the presence of RAFT moieties, and 355 °C for E$_1$ and 335 °C for E$_2$, assigned to the polysaccharide degradation. Grafted copolymers showed just two degradation steps: water loss around 70-90 °C and polysaccharide structure degradation at around 360 °C.
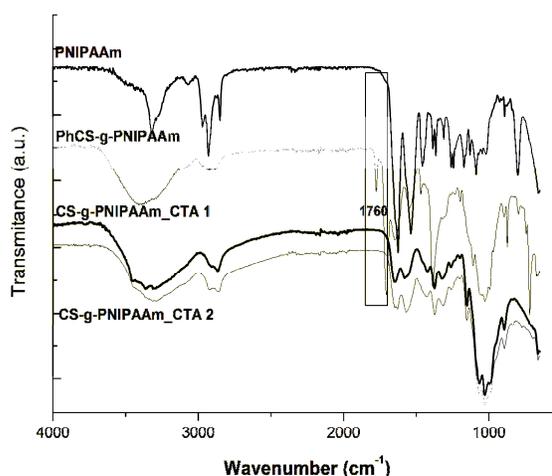


Figure 6: ATR-FT-IR spectra of CS-*g*-PNIPAAm copolymers; CS-*g*-PNIPAAm by using CTA1 and CTA2 pathway synthesis, after deprotection
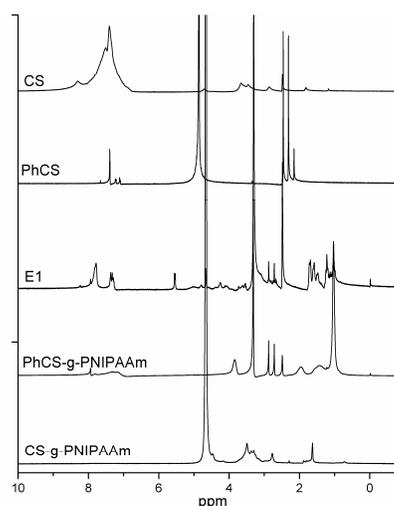


Figure 7: $^1$H-NMR spectra of PhCS-*g*-PNIPAAm copolymer and intermediaries
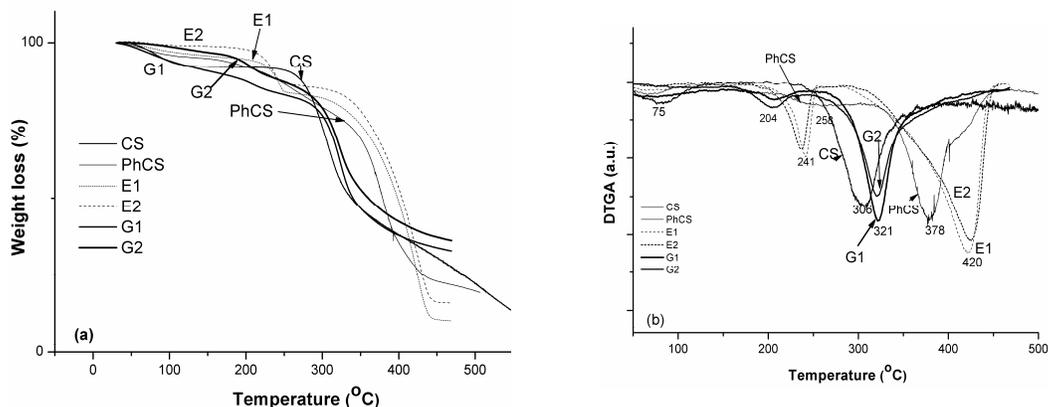
Figure 8: TGA/DTGA curves for functionalized derivatives of chitosan by RAFT polymerization;
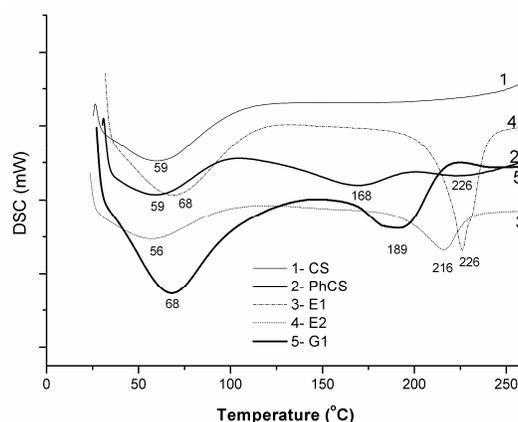(a) TGA curves and (b) first order derivative of TGA curves – DTGA



Figure 9: DSC curves of chitosan and modified chitosan by RAFT

As observed, in Figure 8 (a and b), the two chain transfer agents used to synthesize esters of chitosan and further the grafted copolymers led to similar structures. Not only the esters, but also the graft copolymers showed similar degradation curves, leading to the conclusion that both CTA agents could be successfully used in this type of chemical modification of chitosan.

The DSC curves of chitosan and modified chitosan by RAFT polymerization are shown in Figure 9. As can be seen from Figure 9, the main thermal events are those corresponding to water and moisture losses, between 50 to 74 °C; the peak was shifted to higher temperatures as the molecules became more complex. With the modification of chitosan into phthaloyl chitosan, two new thermal events appeared – two small endothermic peaks, which can be attributed to the decomposition of the phthaloyl groups, followed by the polysaccharide chains.

With the addition of the RAFT agent to the phthaloyl chitosan structure, forming ester bonds, a single sharp endothermic peak, like a melting peak around 215-217 °C, was observed. It can be interpreted that the newly formed ester has a homogenous structure and this is the point it degrades. The polymerization of NIPAAm with chitosan macro-CTA ended up in a compound, which, except for the water and moisture loss that shifted from 56 °C to 67 °C, did not show any other important thermal event as a result of the formation of a homogenous and amorphous structure. DSC results were found to be comparable with the TGA results.
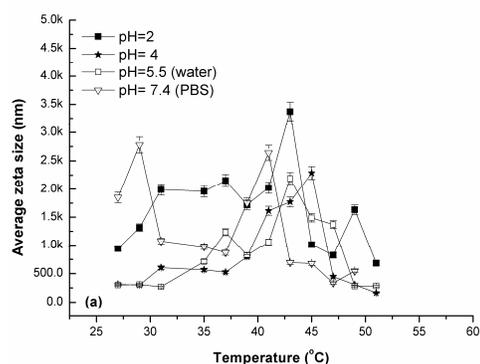
**Responsive behaviour of CS-*g*-PNIPAAm**

The responsive behaviour of the final product synthesized by the RAFT method, *i.e.* CS-*g*-PNIPAAm, was verified by means of particle size analysis within the temperature range from 25 to

8

55 °C. The temperature range was chosen on the basis of PNIPAAm characteristics, as its LCST is known to be of 32 °C. By measuring the particle size of the aqueous solution of the graft copolymer, it was observed that it increased with increasing temperature. Furthermore, the number of countable species decreased and the PDI increased from 0.5 to over 1 (measured within the detection limit of the device). This means that, with increasing temperature, there was a tendency for the particles to associate together, forming agglomerates and the suspension became more non-homogenous.

Moreover, the average particle size was measured, for each temperature, within the range of 25-55 °C (as presented in Fig. 10a) and the critical solution temperature (LCST), where a drastic change in size occurs, was determined. The particle size of the copolymer solutions increased from 500 nm to 3.5 μm, with increasing the temperature from 25 to 50 °C.

By plotting each curve from Figure10 a and applying the sigmoidal mathematical model of Origin graphical program, for each set of measurements, at different pHs, a distinct LCST value was obtained. By plotting the obtained LCST values of the graft copolymer solutions with different pHs, it was observed that LCST shifted to lower temperatures with increasing pH (Fig. 10b). In the physiological medium (pH 7), where the controlled delivery takes place, an LCST of the solution of 40 °C was determined.

Thermal stability, together with the ability to respond to pH and temperature, allowed the use of CS-*g*-PNIPAAm as part of a hydrogel pharmaceutical formulation for topical application.[17] Hydrogels based on Cs-*g*-PNIPAAm presented, alongside pH and temperature responsivity, bioadhesivity and non-toxicity, thus being suitable for topical drug delivery systems. Other modified chitosan based hydrogels were also found suitable for topical application, the evidence being the number of studies performed in this field.[17-20]
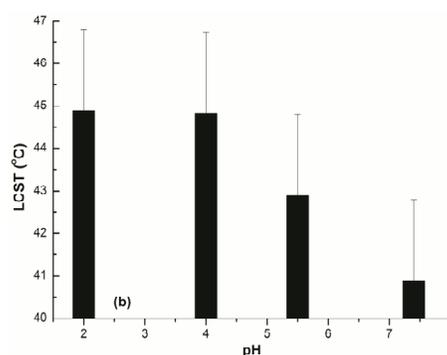


Figure 10: Average zeta size as a function of temperature (a), and dependence of LCST of grafted copolymer solutions on solution pH (b)

**CONCLUSION**

Grafted copolymers of chitosan and poly(N-isopropylacrylamide) (PNIPAAm) were synthesized *via* the RAFT polymerization technique. The "grafting from" method followed a mechanism by which the monomer was polymerized *in situ*, in the presence of a chitosan-macro RAFT agent, synthesized prior to the copolymerization. The study proposed two CTA agents, which had not been used before in this type of reactions, but which are compatible with the monomer as the RAFT methods requires and which offer an alternative for the commonly used AIBN, which rises toxicological issues.

Parallel syntheses were performed and intermediaries were obtained, which gave as final product a copolymer with similar structural and physical-chemical characteristics. After every step, the functionalization efficiency was assessed by FT-IR and ^{1}H-NMR spectroscopy, and the final CS-*g*-PNIPAAm copolymers were obtained with a grafting efficiency of 36%.

Additionally, thermal analyses revealed that, with the modification of the chitosan backbone by

attaching protective groups and then the CTA groups, the structure became more complex and more resistant to thermal decomposition. The thermal degradation (TGA) and DSC curves of the final copolymer showed a more complex polymeric structure, which was more thermally stable, compared to simple chitosan.

The newly synthesized copolymer was tested and it showed water solubility and temperature responsivity. The particle size of the copolymer solution increased with increasing temperature and a tendency for the particles to associate together, forming agglomerates, was observed, the suspension becoming more non-homogenous. An LCST of the solution of 38-42 °C was determined.

The CS-*g*-PNIPAAm copolymer can be used in the preparation of various pharmaceutical formulations for topical applications, as hydrogel, solution or solid.

**REFERENCES**
[1] J. Chiefari, F. Chong Ercole, J. Krstina, J. Jeffery, T. P. T. Le *et al*., *Macromolecules*, **31**, 5559 (1998), https://doi.org/10.1021/ma9804951
[2] C. N. Cheaburu-Yilmaz, S. Y. Karavana and O. Yilmaz, *Curr. Org. Synth.*, **14**, 1 (2017), https://doi.org/10.2174/1570179414666161115150818
[3] W. M. Argüelles-Monal, J. Lizardi-Mendoza, D. Fernández-Quiroz, M. T. Recillas-Mota and M. Montiel-Herrera, *Polymers*, **10**, 342 (2018), https://doi.org/10.3390/polym10030342
[4] C. N. Cheaburu-Yilmaz, S. Y. Karavana and O. Yilmaz, in *AIP Conf. Procs.*, **1918**, 020009 (2017), https://doi.org/10.1063/1.5018504
[5] C. N. Cheaburu-Yilmaz, O. Yilmaz and C. Vasile, *Adv. Struct. Mater.*, **74**, 341 (2015), https://doi.org/10.1007/978-81-322-2473-0_11
[6] J. B. McLeary, F. M. Calitz, J. M. McKenzie, M. P. Tonge, R. D. Sanderson *et al*., *Macromolecules*, **38**, 3151 (2005), https://doi.org/10.1021/ma047696r
[7] D. Hua, J. Tang, J. Cheng, W. Deng and X. Zhu, *Carbohyd. Polym.*, **73**, 98 (2008), https://doi.org/10.1016/j.carbpol.2007.11.008
[8] K. Zhang, Z. Wang, Y. Li, Z. Jiang, Q. Hu *et al*., *Carbohyd. Polym.*, **92**, 662 (2013), https://doi.org/10.1016/j.carbpol.2012.09.003
[9] J. Tang, D. Hua, J. Cheng, J. Jiang and X. Zhu, *Int. J. Biol. Macromol.*, **43**, 383 (2008), https://doi.org/10.1016/j.ijbiomac.2008.07.019
[10] J. Jiang, D. Hua and J. Tang, *Int. J. Biol. Macromol.*, **46**, 126 (2010), https://doi.org/10.1016/j.ijbiomac.2009.10.008
[11] J. Jiang, X. Pan, J. Cao, J. Jiang, D. Hua *et al*., *Int. J. Biol. Macromol.*, **50**, 586 (2012), https://doi.org/10.1016/j.ijbiomac.2012.01.033
[12] D. Hua, J. Jiang, L. Kuang, J. Jiang, W. Zheng *et al*., *Macromolecules*, **44**, 1298 (2011), https://doi.org/10.1021/ma102568p
[13] K. Kurita, H. Ikeda, Y. Yoshida, M. Shimojoh and M. Harata, *Biomacromolecules*, **3**, 1 (2002), https://doi.org/10.1021/bm0101163
[14] C. N. Cheaburu-Yilmaz, S. Y. Karavana and O. Yilmaz, in *Procs. 21ᵗʰ Int. Conf. Inventics*, Iasi, Romania, pp. 37-46, 2017
[15] I. Rodríguez-Sanchez, E. A. Zaragoza-Contreras and D. Glossman-Mitnik, *J. Mol. Mod.*, **16**, 95 (2010), https://doi.org/10.1007/s00894-009-0524-z
[16] M. Lavertu, Z. Xia, A. N. Serreqi, M. Berrada, A. Rodrigues *et al*., *J. Pharm. Biomed. Anal.*, **32**, 1149 (2003), https://doi.org/10.1016/S0731-7085(03)00155-9
[17] C. N. Cheaburu-Yilmaz, O. Yilmaz, F. Aydin Kose and N. Bibire, *Polymers*, **11**, 1432 (2019), https://doi.org/10.3390/polym11091432
[18] I. P. Merlusca, C. Ibanescu, C. Tuchilus, M. Danu, L. I. Atanase *et al*., *Cellulose Chem. Technol.*, **53**, 709 (2018), http://www.cellulosechemtechnol.ro/pdf/CCT7-8(2019)/p.709-719.pdf
[19] S. Rençber, C. N. Cheaburu-Yilmaz, F. A. Köse, S. Y. Karavana and O. Yilmaz, *Cellulose Chem. Technol.*, **53**, 655 (2019), https://doi.org/10.35812/CelluloseChemTechnol.2019.53.64
[20] M. Popa, B. C. Ciobanu, L. Ochiuz, J. Desbrieres, C. S. Stan *et al*., *Cellulose Chem. Technol.*, **52**, 353 (2018), http://www.cellulosechemtechnol.ro/pdf/CCT5-6(2018)/p.353-370.pdf